

## Original Research

## Comparative study of radiomics, tumor morphology, and clinicopathological factors in predicting overall survival of patients with rectal cancer before surgery

Zhou Chuanji<sup>1</sup>, Wang Zheng<sup>1</sup>, Lai Shaolv<sup>\*</sup>, Meng Linghou, Lu Yixin, Lu Xinhui, Lin Ling, Tang Yunjing, Zhang Shilai, Mo Shaozhou, Zhang Boyang

Department of Radiology, Guangxi Medical University Cancer Hospital, Nanning, Guangxi 530021, China



## ARTICLE INFO

## Keywords:

Magnetic resonance imaging  
Rectal cancer  
Prognosis  
Radiomics  
Tumor morphology  
Nomogram  
Overall survival

## ABSTRACT

We compared the ability of a radiomics model, morphological imaging model, and clinicopathological risk model to predict 3-year overall survival (OS) in 206 patients with rectal cancer who underwent radical surgery and had magnetic resonance imaging, clinicopathological, and OS data available. The patients were randomized to a training cohort ( $n = 146$ ) and a verification cohort ( $n = 60$ ). Radiomics features were extracted from preoperative T2-weighted images, and a radiomics score model was constructed. Factors that were significant in the Cox multivariate analysis were used to construct the final morphological tumor model and clinicopathological model. A comprehensive model in the form of a line chart was established by combining the three models. Ten radiomics features significantly related to OS were selected to construct the radiomics feature model and calculate the radiomics score. In the morphological model, mesorectal extension depth and distance between the lower tumor margin and the anal margin were significant prognostic factors. N stage was the only significant clinicopathological factor. The comprehensive model combined with the above factors had the best prediction performance for OS. The C-index had a predictive performance of 0.872 (95% confidence interval [CI]: 0.832–0.912) in the training cohort and 0.944 (95% CI: 0.890–0.990) in the verification cohort, which was better than for any single model. The comprehensive model was divided into high-risk and low-risk groups. Kaplan-Meier curve analysis showed that all factors were significantly correlated with poor OS in the high-risk group. A comprehensive nomogram based on multi-model radiomics features can predict 3-year OS after rectal cancer surgery.

## Introduction

Colorectal cancer is the third most common malignancy worldwide, in which the incidence of rectal cancer is higher than that of colon cancer. In recent years, rectal cancer in China has been characterized by low age, high middle and lower rectum incidence, and locally advanced stage [1]. Its complications, mortality, adverse treatment-related reactions, and associated medical expenses impose a substantial societal burden worldwide. However, the incidence of and mortality from cancer varies according to the societal environment. In a recent international

epidemiological study by Wong et al. [2], the morbidity and mortality associated with rectal cancer have increased more in countries with a high human development index (HDI), that is, countries undergoing rapid economic and societal changes than in those with a low human development index. Moreover, rectal cancer incidence is on the rise among young and middle-aged people under 50 years, especially in adult women [3,4]. Although comprehensive perioperative therapy with surgery as the core treatment can significantly improve the local radical resection rate, effectively reduce the likelihood of local recurrence, and prolong postoperative survival in patients with rectal tumors, the overall

*Abbreviation:* MRI, magnetic resonance imaging; LASSO, least absolute shrinkage and selection operator; HDI, human development index; CEA, carcinoembryonic antigen; CA199, carbohydrate antigen-199; LVI, lymphovascular invasion; PNI, perineural invasion; TD, tumor deposits; MED, mesorectal extension depth; CRM, circumferential resection margin; OS, overall survival; VOIs, volume of interests; LoG, Laplacian of Gaussian; ICC, interclass correlation coefficient; DCA, decision curve analysis; ROC, receiver-operating characteristic; AUC, area under the receiver-operating characteristic curve.

<sup>\*</sup> Corresponding author.

E-mail address: [LSL1688@139.com](mailto:LSL1688@139.com) (L. Shaolv).

<sup>1</sup> Zhou Chuanji and Wang Zheng contribute equally to the article.

<https://doi.org/10.1016/j.tranon.2022.101352>

Received 7 October 2021; Received in revised form 26 December 2021; Accepted 19 January 2022

1936-5233/© 2022 The Authors. Published by Elsevier Inc. This is an open access article under the CC BY-NC-ND license

(<http://creativecommons.org/licenses/by-nc-nd/4.0/>).

prognosis is poor. Therefore, effective methods for predicting and improving overall survival (OS) and quality of life have become an urgent concern for both doctors and patients [5,6].

In clinical practice, predicting survival in patients with rectal cancer is mostly based on the TNM staging system, which is widely used in all aspects of diagnosis and treatment of cancer. However, although it includes the degree of local invasion, regional lymph node involvement, and distant organ metastasis, the TNM staging system cannot accurately reflect biological differences in stages of tumor diagnosis and treatment [7–9]. The clinical significance of identifying prognostic features that would give clinicians the choice of the best individual treatment and provide a quantitative parameter for the prognosis in patients who undergo surgery for rectal cancer is self-evident [6,10,11]. Imaging is a rapid, convenient, and non-invasive examination method that has long been the first choice for rectal cancer staging, predicting the curative effect of treatment and follow-up after treatment. Magnetic resonance imaging (MRI), MRI defecography, computed tomography (CT), and positron emission tomography-CT (PET/CT) are important imaging techniques for rectal cancer. Notably, studies have shown that changes in Pet/ct SUVmax may indicate the antitumor activity of different drugs and therapeutic agents at different time points and may guide the choice of new therapeutic doses in the future [12–14]. Although most of these techniques allow morphological observation of a tumor, they do not provide quantitative information reflecting changes in microcosm heterogeneity within the tumor. The biological characteristics of a lesion have limited prognostic ability [9,15–17].

Radiomics offers a new perspective for both doctors and patients in that it can extract quantitative information from morphological and functional images and mine for further parameters and features that reflect the histopathological and physiological characteristics of tumors, thereby serving as a valuable tool for clinical diagnosis and treatment, research, and reference purposes. Radiomics can be used in both normal and abnormal human tissues [15,18] and has been widely used for predicting biological characteristics, assessing the potential curative effects of treatment, and therapeutic decision-making in rectal cancer [19–23]. Radiomics analysis has also been successfully used to predict survival outcomes in other diseases [18,23–27].

Most of the previous studies on the prognosis of rectal cancer have concluded that a combination of clinicopathological and radiological features is superior to a single biomarker in terms of prognostic ability [21–23,27]. Therefore, this study compared the ability of a morphological imaging model, a radiomics model, and a clinicopathological risk model to predict the 3-year OS of patients with rectal cancer.

## Materials and methods

### Patient data

The study was approved by the Ethics Review Committee of the Affiliated Cancer Hospital of Guangxi Medical University. All patients provided written informed consent. Patients with rectal cancer diagnosed in the anorectal surgery ward of the Affiliated Cancer Hospital of Guangxi Medical University between January 1, 2016, and April 30, 2018, were included. The baseline patient characteristics obtained included clinical data, demographic characteristics, laboratory results, pre-treatment MRI data, pathological results, and survival outcomes. All patients met the following inclusion criteria: (1) rectal cancer confirmed by pathology; (2) contrast-enhanced rectal MRI performed within 2 weeks before surgery; and (3) radical rectal surgery performed. The exclusion criteria were as follows: (1) neoadjuvant chemotherapy or radiotherapy before surgery; (2) another cancer diagnosis; (3) incomplete MRI or image quality that was too poor to be used for image segmentation and extraction and analysis of radiological features; and (4) missing clinical, laboratory, or pathological data. Finally, 206 patients (mean age  $59.72 \pm 11.56$  years) were randomized to a training cohort ( $n = 146$ ) and a validation cohort ( $n = 60$ ) at a ratio of 7:3.

### Treatment and follow-up

All patients underwent radical rectal resection and received adjuvant treatment after surgery. Regular follow-up was performed every 3–6 months in the first 2 years, and every 6 months in the third year. The main study endpoint was 3-year OS, either from the date of operation to death of any cause or survival in 36 months. A nomogram was established according to the 3-year OS.

### MRI imaging acquisition

Patients were examined by MRI within 2 weeks before the operation. Baseline MRI data were obtained on 3.0T GE equipment (DISCOVERY MR750W GEHC) using the body phase control line coil with 16 channels. Before the examination, an intestinal preparation required includes a liquid diet on the day before the scan and an empty stomach on the day of the scan. Anisodamine of 10 mg was injected intramuscularly 15 min before the scan to inhibit gastrointestinal peristalsis. Scan sequence and parameters include T2WI that uses axial fast spin echo sequence, TE 102 ms, FOV  $18.0 \times 18.0$  mm, matrix  $288 \times 256$ , layer thickness 3.0 mm, layer spacing 0.3 mm.

### Research methods

#### MRI morphological measurements

The patients were evaluated in the transverse section, sagittal section, coronal section, and oblique axial planes and with T1-weighted, T2-weighted, and T1-weighted contrast enhancement sequences; the cancers were most clearly shown on T2-weighted images (T2WI). The MRI scans were independently read and evaluated by two radiologists with extensive experience in diagnostic imaging of the gastrointestinal tract who were blinded to all data on pathology. In the event of disagreement, a consensus was reached by discussion (Fig. 1).

The morphological indices measured in this study were as follows and are summarized in Fig. 2.

*Distance between the lower tumor margin and the anal margin.* First, look for the lowest edge of the tumor on the sagittal section, and then measure the distance from the lower edge of the tumor to the anal margin along the central axis of the rectum. If the tumor invades the perianal region, the distance is 0. To improve readability, the "tumor position," namely, the distance between the lower tumor margin and the anal margin, was recorded.

*Longitudinal length of tumor involvement.* The longitudinal length of tumor involvement was measured in the sagittal section along the central axis of the rectum. If the tumor was discontinuous, the lengths were measured separately and then added.

*Maximum tumor diameter.* The largest section of the tumor was found on the oblique axial position (perpendicular to the tumor line and scanned by MRI). The tumor was measured in a straight line perpendicular to the intestinal wall from the outer edge of the tumor. This measurement should not be performed in the conventional axial position. When the direction of the intestinal canal where the tumor is located is not perpendicular to the central axis of the human body, the scanning direction obliquely scans the focus of the tumor, resulting in a deviation in the shape of the tumor.

*Ratio of tumor circumference to intestinal wall circumference.* The ratio of the circumferential length of the intestinal wall to the total perimeter of the intestinal wall was calculated by measuring the circumferential ratio of the tumor to the intestinal wall on the oblique axis and calculating the ratio of the circumferential length of the invaded intestinal wall to the total perimeter of the intestinal wall. This value can be divided into

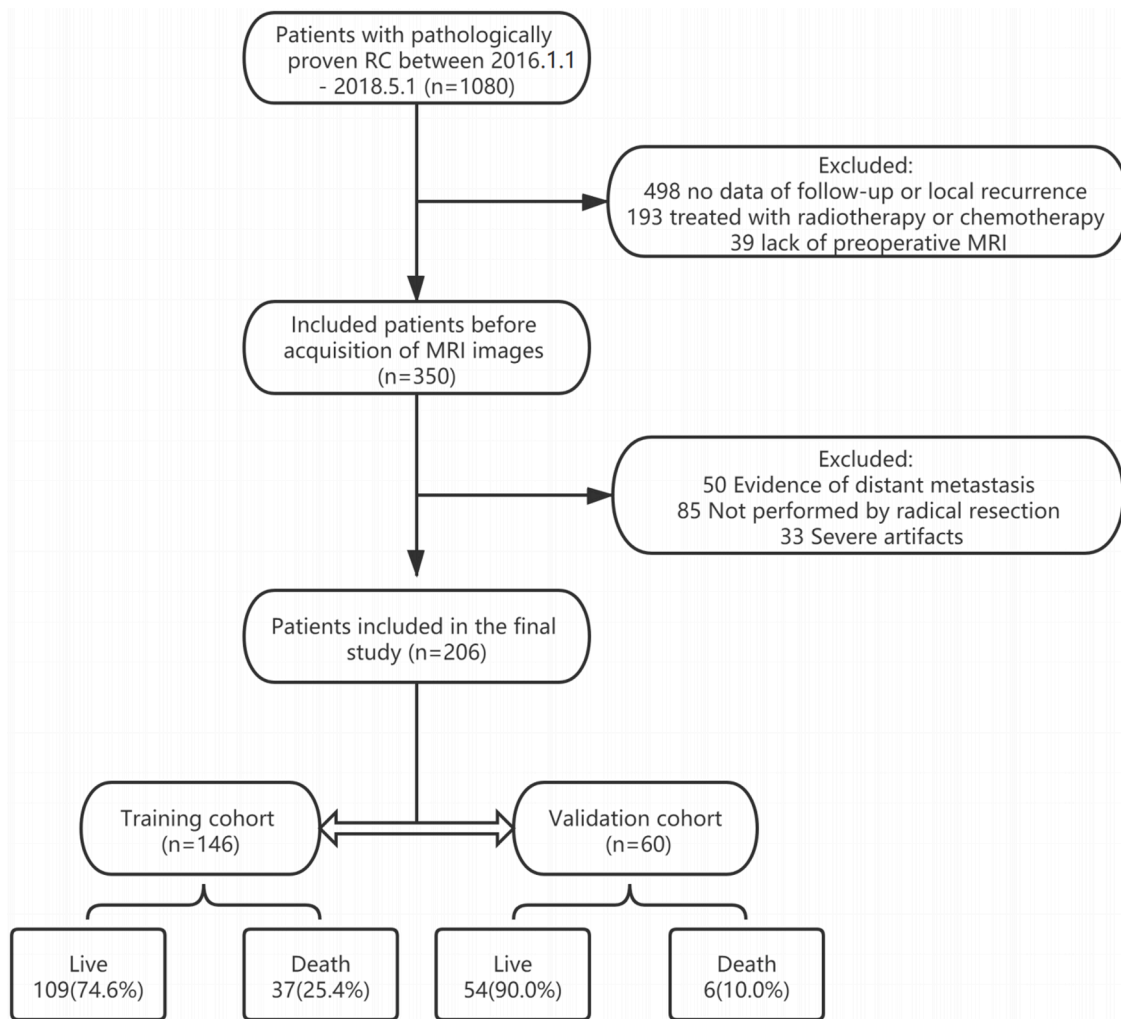


Fig. 1. Flow chart of the recruitment pathway for patients included in the study.

0–25%, 26–50%, 51–75%, and 76–100%.

**Mesorectal extension depth (MED).** The maximum distance from the outer edge of the low-signal muscular layer to the outermost edge of the tumor in the mesorectum was measured on the oblique axis. This signal is usually similar to a tumor signal. At this time, the tumor was stage T3 or T4. If the muscular layer is destroyed or unclear, the line between the adjacent muscular layers is used as the temporary line, which is regarded as the outer boundary of the muscular layer.

**Circumferential resection margin (CRM).** In order to avoid observation errors, the distance between the tumor margin, metastatic lymph nodes, or tumor deposits and the mesorectal fascia is  $< 1$  mm or mesorectum fascia invasion, interruption, and enhancement, the circumferential incisional margin is considered to be positive.

**Calculation of tumor volume.** After calculating the length, width, and height of each pixel block in the ROI, the volume of a single-pixel block was obtained. Finally, the volume of all pixel blocks in the ROI was added to obtain the volume of the entire tumor.

#### Radiomics

**Radiomics analysis.** The workflow for the radiomics analysis included four steps: segmentation of tumor images, extraction of radiomics features, selection of features, and model building (Fig. 3).

**Tumor image segmentation.** Open source software ITK-SNAP ([www.itk-snap.org](http://www.itk-snap.org)) was used to manually draw the oblique axis on the T2WI. Although radiomics features can be extracted from a two-dimensional region of interest (ROI) or a three-dimensional voxel of interest, “ROI” was chosen to represent both to improve readability. The ROI was interpreted by two radiologists with more than 3 years of experience in diagnostic MRI for gastrointestinal diseases, who manually outlined the ROI of the rectal tumor at each level. The tumor area was defined as a slightly higher signal on T2WI, which was different from the adjacent intestinal wall. The final decision was made by a senior radiologist with 8 years of experience in segmentation validation and calculating intraclass correlation coefficients (ICC).

**Extraction of radiomics features.** T2WI is an essential sequence included in the standard rectal MR protocol, and it is also the most important one for the assessment and local staging of rectal cancer. Because it offers good visualization of rectal wall layers and provides good contrast between tumor, surrounding fat, and mesorectal fascia, indicating a better appearance and feature stability [28,29]. In the predictive model constructed by Liang et al. to predict metachronous liver metastasis in patients with rectal cancer, the best model is the feature parameters extracted based on the T2WI sequence [30].

After the tumor ROI was segmented manually, the T2WI image was normalized using the Z-score. The image resampling voxel is in the standardized intensity range of  $3 \times 3 \times 3$  mm, and the gray level of each layer image is quantized to 25 gray levels. The aim is to reduce as far as

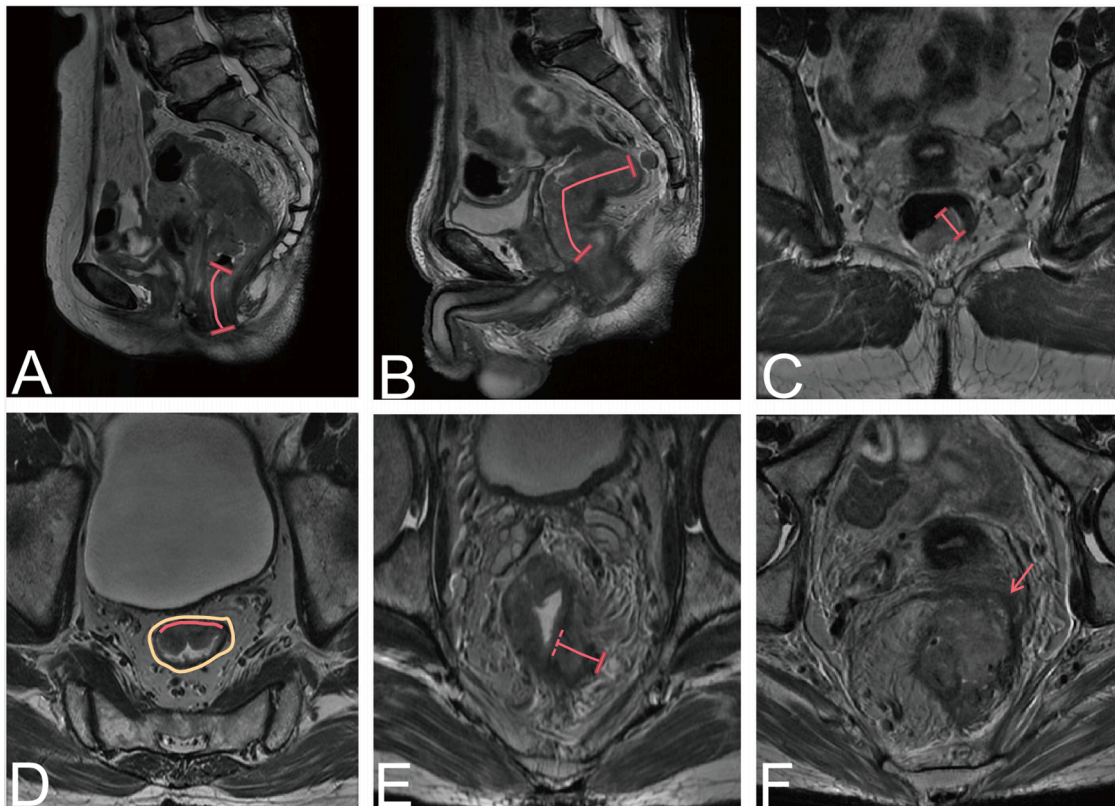


**Fig. 2.** Tumor morphology detected on magnetic resonance images. (A) Distance from the lower margin of the tumor to the anal margin. (B) Length of tumor involvement. (C) Maximum tumor diameter. (D) The proportion of the tumor in relation to the circumference of the intestinal wall. The red line outlines part of the tumor, and the brown color represents the whole intestinal wall. (E) Depth of tumor invasion to the mesorectum. (F) Involvement of the circumferential resection margin (red arrow). (For interpretation of the references to color in this figure legend, the reader is referred to the web version of this article.)

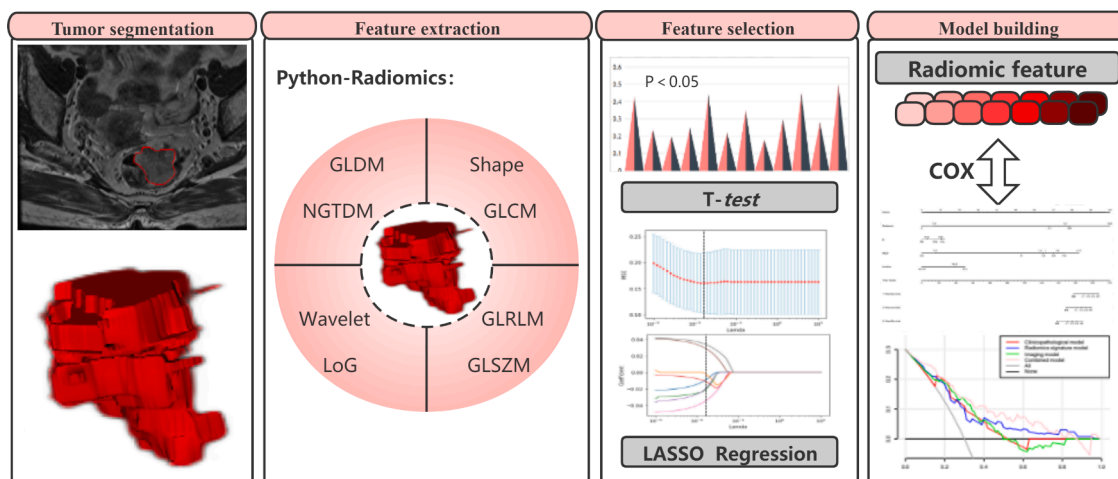


**Fig. 3.** Radiomics framework for predicting overall survival in patients with rectal cancer.

possible any drift in image intensity caused by the use of different inspection equipment and scanning parameters, the influence of inconsistency between images, and the difference in voxels between images. The smaller the difference, the better the effect. It is more convenient to use convolution operations to extract common features. Finally, the “Radiomics” package [31] of the open source Python software was used to extract radiomics features from T2WI and the ROI.

For each case, we extracted a total of 1781 radiomics features, 107 of which were in the original images. Seven filters were used to extract these features: (1) wavelet ( $n = 744$ ): MR images can be divided

according to whether they are high-frequency or low-frequency, and first-order and second-order features can be extracted for each frequency range, which helps quantify high-dimensional and multi-frequency information that is difficult to observe with the naked eye; (2) Laplacian of Gaussian (LoG,  $n = 465$ ), which emphasizes a region of change in gray value, calculates the fineness (short-distance gray variation) and roughness (long-distance gray variation) of texture features, and then analyzes the multi-scale spatial information for the tumor, providing a tumor texture analysis model that is both detailed and macroscopic; (3) logarithmic ( $n = 93$ ); (4) exponential ( $n = 93$ ); (5)

square ( $n = 93$ ); (6) square root ( $n = 93$ ); and (7) gradient ( $n = 93$ ) [20, 24].

The features finally extracted were as follows: (1) first-order statistics ( $n = 19$ ); (2) shape ( $n = 16$ ); (3) gray-level co-occurrence matrix (GLCM,  $n = 24$ ); (4) gray-level dependence matrix (GLDM,  $n = 14$ ); (5) gray-level size zone matrix (GLSZM,  $n = 16$ ); (6) neighboring gray tone difference matrix (NGTDM,  $n = 5$ ); and (7) gray-level run length matrix (GLRLM,  $n = 16$ ) [18,31].

**Selection of radiomics features.** Although radiomics features reflect biological information for a tumor from multiple angles, not all biological information is related to OS in patients with rectal cancer. Therefore, survival and death groups are used as cutpoints for feature reduction and screening in this study. A two-step feature selection method is adopted to retain only the strongest features significantly related to OS. First, we calculated the  $P$ -value for each feature as a predictor of OS in the training cohort using the  $t$ -test and selected features with a  $P$ -value of  $< 0.05$  as meaningful candidate prognostic factors ( $n = 44$ ). A least absolute shrinkage and selection operator (LASSO) logistic analysis was then performed to determine the most useful prognostic features. LASSO-logistic regression is a method used to select variables for a linear regression model and controls the number of selected features by imposing a constraint on the  $\lambda$  parameter. This constraint causes the regression coefficient of some variables to shrink to zero; variables with a zero regression coefficient are excluded from the model, which not only compresses the insignificant variable coefficient to zero to select the variable with a non-zero regression coefficient. In order to obtain the optimal number of features and avoid over-fitting, we performed 10 rounds of cross-validation to select the optimal  $\lambda$  value (Fig. 4A, B) and then used Z-score transformation to standardize all the selected features.

**Statistical analysis**

Univariate and multivariate Cox regression analysis, Kaplan-Meier analysis, and receiver-operating characteristic (ROC) curve analysis were performed using MedCalc 19.7 software (<https://www.medcalc.org>).

Python 3.7 software (<https://www.python.org>) was used for screening and extraction of tumor features. Nomogram construction, C-index calculation, and decision curve analysis (DCA) were performed using R 4.0.5 software (<http://www.R-project.org>). A  $P$ -value  $< 0.05$  was considered statistically significant.

**Results**

*Construction of prediction models*

Four models were constructed: a clinicopathological model, a morphological imaging model, a radiomics features (Rad-score) model, and a comprehensive model (the nomogram). All factors in each model (Table 1) were evaluated using Cox univariate and multivariate analyses (Table 2). All variables that were significant in univariate analysis were subjected to ROC curve analysis, and cutoff values were calculated (Table 2) to identify high-risk and low-risk groups. The performance of each model was then evaluated using the C-index (Table 3) and DCA. The C-index indicates the consistency between the OS predicted by the model and actual patient OS. A C-index of approximately 0.5 indicates poor predictive ability, and a C-index around 0.7 indicates good predictive ability. DCA is used to evaluate the degree of benefit for patients and introduces the concept of “threshold probability.” Under the same threshold probability, the model brings a higher net benefit to patients and is more clinically relevant. The median follow-up duration was 39 months (range, 1–55). There were 37 deaths (mean survival time  $20.7 \pm 10.97$  months) in the training cohort and 6 deaths (mean survival time  $24.0 \pm 8.461$  months) in the validation cohort; the between-group differences were not statistically significant ( $P = 0.351-0.949$ ).

*Ability of the clinicopathological model to predict OS*

Thirteen clinicopathological indices were evaluated, namely, age, sex, carcinoembryonic antigen (CEA), carbohydrate antigen-199 (CA199), TNM stage, cancer nodules (tumor deposits), tumor differentiation, histological type, tumor volume, p53, Ki67, perineural invasion,

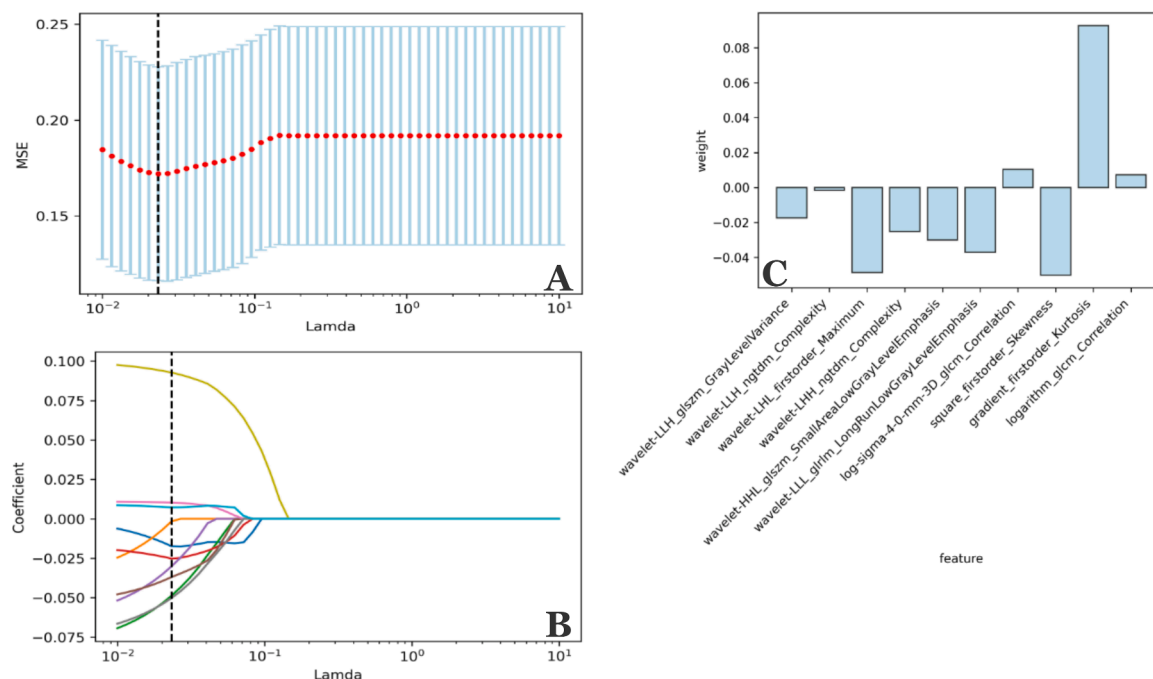


**Fig. 4.** Selection of features based on the LASSO regression model. (A) Adjusting the  $\lambda$  parameter in the LASSO model, with 10 rounds of cross-validation performed to pass the minimum standard. The optimal  $\lambda$  value was  $-0.0233$  and is indicated by the vertical dashed line. (B) A representative LASSO coefficient distribution map. According to the coefficient distribution map generated by the  $\lambda$  sequence, a vertical dashed line is drawn at the value selected after 10 rounds of cross-validation. Ten non-zero coefficients are screened by the best  $\lambda$  value. (C) Coefficient values for the eight features. LASSO, least absolute shrinkage and selection operator.

**Table 1**  
Clinicopathological and Imaging characteristics of patients in the training cohort and validation cohort.

Characteristics	Training cohort (n = 146)	Validation cohort (n = 60)	P Value*
Age(years, mean±SD)	59.7 ± 11.522	58.42±12.057	P = 0.4404
Gender (%)			P = 0.0109*
Male	94(64.4%)	39(65.0%)	
Female	52(35.6%)	21(35.0%)	
CEA(%)			P = 0.9436
≤ 5(Normal)	94(64.4%)	40(66.7%)	
> 5(Abnormal)	52(35.6%)	20(33.3%)	
CA199(%)			P = 0.4931
≤ 37(Normal)	100(68.5%)	39(65.0%)	
> 37(Abnormal)	46(31.5%)	21(35.0%)	
Pathological T stage (%)			P = 0.0016*
T1	7(4.7%)	5(8.3%)	
T2	39(26.8%)	16(26.7%)	
T3	89(61.0%)	35(58.3%)	
T4	11(7.5%)	4(6.7%)	
Pathological N stage (%)			P < 0.0001*
N0	68(46.6%)	35(58.3%)	
N1a	17(11.7%)	5(8.3%)	
N1b	7(4.8%)	7(11.7%)	
N1c	21(14.4%)	6(10.1%)	
N2a	15(10.2%)	2(3.3%)	
n2b	18(12.3%)	5(8.3%)	
Tumor deposits (%)			p = 0.9598
Negative	114(78.1%)	53(88.3%)	
positive	32(21.9%)	7(11.7%)	
Tumor differentiation(%)			p = 0.5540
High	5(3.4%)	1(1.6%)	
Moderate	118(80.9%)	56(93.4%)	
poor	5(15.7%)	3(5.0%)	
Tumor type(%)			p = 0.3503
Mass type	53(36.3%)	20(33.3%)	
Ulcerative type	87(59.6%)	39(65.0%)	
Infiltrating type	6(4.1%)	1(1.7%)	
P53(%, mean±SD)	45±37.98	35±38.84	P = 0.4689
Ki67(%, mean±SD)	77±17.05	71±22.09	P = 0.9175
Pathological LVI (%)			P = 0.3544
Negative	96(65.7%)	46(76.7%)	
Positive	50(34.3%)	14(23.3%)	
Pathological PNI (%)			P = 0.1779
Negative	81(55.5%)	47(78.3%)	
Positive	65(44.5%)	13(21.7%)	
Tumor length(cm, mean±SD)	5.10 ± 2.00	5.14 ± 2.10	P = 0.0023*
Tumor location from anal verge(cm,mean±SD)	6.492 ± 3.3537	6.835 ± 3.6370	P = 0.0027*
MED(cm,mean±SD)	0.50 ± 0.47	0.43 ± 0.38	P = 0.0001*
Tumor diameter(cm, mean±SD)	1.64 ± 0.62	1.64 ± 0.83	P = 0.2649
Tumor proportion of intestinal wall(%)			P = 0.0874
0–25%	2(1.3%)	3(5.0%)	
26–50%	45(30.9%)	17(28.3%)	
51–75%	55(37.6%)	18(30.0%)	
76–100%	44(30.2%)	22(36.7%)	
Tumor volume(cm <sup>3</sup> , mean±SD)	17.47±14.42	18.35±18.07	P = 0.1353
CRM(%)			P = 0.0126*

**Table 1 (continued)**

Characteristics	Training cohort (n = 146)	Validation cohort (n = 60)	P Value*
Negative	137(93.9%)	57(95.0%)	
Positive	9(6.1%)	3(5.0%)	
Overall Survival(%)			
Death(month,mean±SD)	37(25.3%,20.7 ± 10.97)	6(10.0%,24.0 ± 8.461)	
Live	109(74.7%)	54(90.0%)	

Abbreviations: CEA, carcinoembryonic antigen; LVI, lymphovascular invasion; PNI, perineural invasion; CA199, carbohydrate antigen-199; Tumor location from anal verge, the distance between the lower margin of the tumor and the anal margin; MED, mesorectal extension depth; CRM, circumferential resection margin.

and lymphovascular invasion. Univariate Cox regression identified five of these indices (T stage, N stage, and gender) to have significant prognostic value. After ROC analysis, the cutoff values for gender were male (hazard ratio [HR] 2.260, 95% CI: 1.084–4.713), as was a T stage >T2 and an N stage >N0 (hazard ratio [HR] 2.591, 95% CI: 1.585–4.235 and HR 1.621, 95% CI:1.833–1.900, respectively).

The three prognostic indices identified to be statistically significant in the univariate Cox model were entered into the multivariate Cox model, in which only the N stage was significant. Therefore, the N stage was included in the clinicopathological prognostic model for OS in patients with rectal cancer.

#### Observation and construction of the morphological tumor model

Tumor morphological variables that were significant in univariate COX regression analysis were as follows: (1) location of the tumor (cutoff value ≤ 5 cm), meaning that the shorter the distance between the lower margin of the tumor and the anal margin, the higher the mortality risk (HR 1.843, 95% CI: 1.960–15.572); (b) tumor length (cutoff value > 3.75 cm), meaning that the longer the length of the intestinal wall involved, the higher the mortality risk (HR 1.286, 95% CI: 1.133–1.459); (3) mesorectal extension depth (MED, cutoff value > 0.45 cm), meaning that the longer the length of mesorectum invaded by the tumor, the higher the mortality risk (HR 5.511, 95% CI: 3.221–9.430); (4) circumferential resection margin (CRM), meaning that the mortality risk was significantly higher in CRM-positive patients than in CRM-negative patients (HR 2.127, 95% CI: 1.027–4.403). These five significant univariate variables were then incorporated into the multivariate Cox regression analysis, in which only tumor location and MED remained statistically significant (P = 0.01 and P = 0.02, respectively, paired t-test). Therefore, these two variables were included in the morphological model to predict OS in patients with rectal cancer.

#### Construction of the radiomics scoring model

A total of 1781 radiomics features were extracted from T2WI for each subject. Using a series of selection operations, including LASSO, ten radiomics features were identified to have a statistically significant impact on OS: (1) wavelet-LLH\_glszm\_GrayLevelVariance; (2) wavelet-LLH\_ngtdm\_Complexity; (3) wavelet-LHL\_firstorder\_Maximum; (4) wavelet-LHH\_ngtdm\_Complexity; (5) wavelet-HHL\_glszm\_SmallArea LowGrayLevelEmphasis; (6) wavelet-LLL\_glrml\_LongRunLowGrayLevel Emphasis; (7) log-sigma-4-0-mm-3D\_glcm\_Correlation;(8)square\_first-order\_Skewness;(9) gradient\_firstorder\_Kurtosis; and (10) logarithm\_glcm\_Correlation. The filter was composed of wavelet (n = 6), LoG (n = 1), square (n = 1), gradient (n = 1), and logarithm(n = 1). The feature categories were first-order (n = 3), GLSZM (n = 2), NGTDM (n = 2), GLRLM(n = 1), and GLCM (n = 2). The coefficients for each feature are shown in Fig. 4C. Next, these eight key features were used to calculate the radiomics score (Rad-score) using the following formula:

**Table 2**  
Univariate and multivariate analysis of OS in the total patient.

Characteristics	Univariate analysis			Multivariate analysis	
	Hazard ratio (95% CI)	Cutoff	P Value	Hazard ratio (95% CI)	P Value
Gender (Male vs. Female)	2.260(1.084–4.713)		0.02		
CRM (Negative vs. Positive)	2.127(1.027–4.403)		0.042		
Tumor length (cm, high vs. low)	1.286(1.133–1.459)	> 3.75	0.007		
Pathological T stage	2.591(1.585–4.235)	> T2	0.001		
Pathological N stage	1.621(1.833–1.900)	> N0	< 0.001	1.40971.164–1.707)	0.004
Tumor location from anal verge (cm, high vs. low)	1.843(1.960–15.572)	≤ 5	0.001	0.839(0.741–0.950)	0.006
MED (cm, high vs. low)	5.511(3.221–9.430)	> 0.45	< 0.001	2.091(1.031–4.243)	0.004
Radscore (low vs. high)	29.605(8.660–101.2)	> -0.02	<0.001	17.518(3.091–99.272)	0.001

**Table 3**  
Performance of models.

Models	AUC (95%CI)		C-index (95%CI)		P Value
	Training+validation cohort	Validation cohort	Training cohort	Validation cohort	
Clinicopathological model	0.772(0.717–0.827)	0.720(0.517–0.923)	0.768(0.713–0.818)	0.720(0.517–0.923)	Vs. Combined model P = 0.0014 P = 0.0169 P = 0.0023
Radiomics signature model	0.826(0.782–0.869)	0.847(0.780–0.934)	0.809(0.757–0.861)	0.847(0.780–0.934)	
Imaging model	0.800(0.746–0.854)	0.835(0.691–0.979)	0.793(0.733–0.853)	0.835(0.691–0.979)	
Combined model	0.882(0.852–0.912)	0.944(0.890–0.990)	0.872(0.832–0.912)	0.944(0.890–0.990)	

**Abbreviations:** CI, confidence interval; Radiomics signature, signature from T2WI.

Rad-score =  $-0.0174 \times \text{feature 1} - 0.0015 \times \text{feature 2} - 0.0487 \times \text{feature 3} - 0.0252 \times \text{feature 4} - 0.0251 \times \text{feature 5} - 0.0369 \times \text{feature 6} + 0.0104 \times \text{feature 7} - 0.0502 \times \text{feature 8} + 0.0927 \times \text{feature 9} + 0.0072 \times \text{feature 10}$ .

A lower Rad-score means a relatively lower risk of death, which means OS is longer, whereas a higher Rad-score indicates a higher risk of death and a relatively short OS. The final average Rad-score was  $-0.0363$  (minimum value  $-0.5$ , maximum value  $0.7$ ). The cutoff Rad-score was calculated to be  $-0.02$  and used to allocate each patient with rectal cancer to a high-risk or low-risk group; the cutoff value for each patient is shown in Fig. 5. The agreement between the two radiologists on the selected radiological characteristics was considered good (ICC range:  $0.779-0.894$ ,  $P < 0.05$ ). COX regression analysis of the Rad-score showed that both single factors and multiple factors were significant ( $P < 0.001$  and  $P = 0.001$ , respectively), and a T2WI-based radiomics signature model was constructed.

#### Development and validation of the comprehensive model

The above models were combined to construct a comprehensive

nomogram (Fig. 6A), including the N stage, the Rad-score, tumor location, and the MED. The line chart assigns each influencing factor, adds each factor score to obtain the total score, and finally draws a line to the risk axis to determine the probability of survival. A higher total score was associated with greater mortality risk. The C-index for the ability of the comprehensive model to predict OS was  $0.872$  (95% CI  $0.852-0.912$ ) in the training cohort and  $0.944$  (95% CI  $0.890-0.990$ ) in the validation cohort, which was better than that of any single model (Table 3). There were significant differences between the comprehensive model and the other three models ( $P < 0.05$ ). The calibration curve for 1–3-year OS (Fig. 6B, C) indicates good accuracy between prediction and actual observation of the training and validation groups. Time-independent ROC analysis confirmed that the comprehensive model had the best prognostic ability. DCA (Fig. 7A) showed two lines of reference: A black line for all that is alive and a gray slash for all that is dead. The closer the model curves are to these two reference lines, the less useful they are. In most reasonable threshold probability ranges, the comprehensive model was superior to the clinicopathological, morphological, and radiological models and would be of the most clinical benefit.

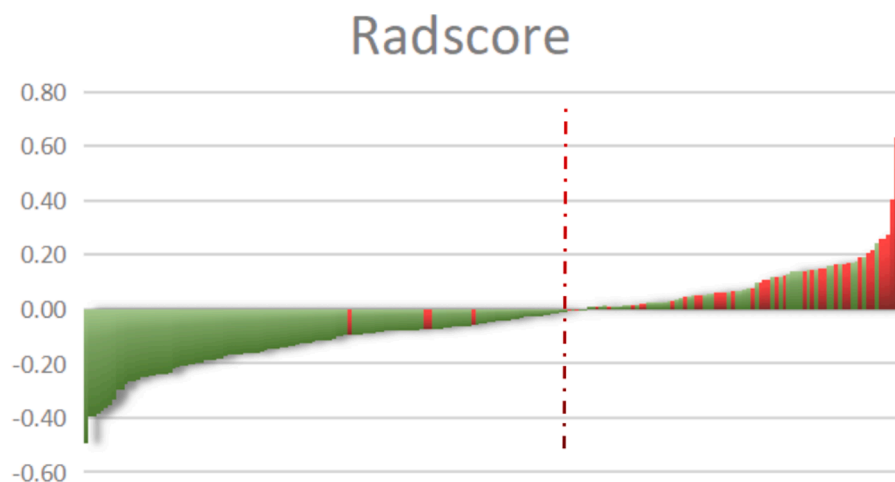


**Fig. 5.** Rad-scores for each patient with rectal cancer. Green indicates that the patient survived and red indicates that the patient died. The red dotted line indicates the Rad-score. The higher this score, the greater the chance of death.

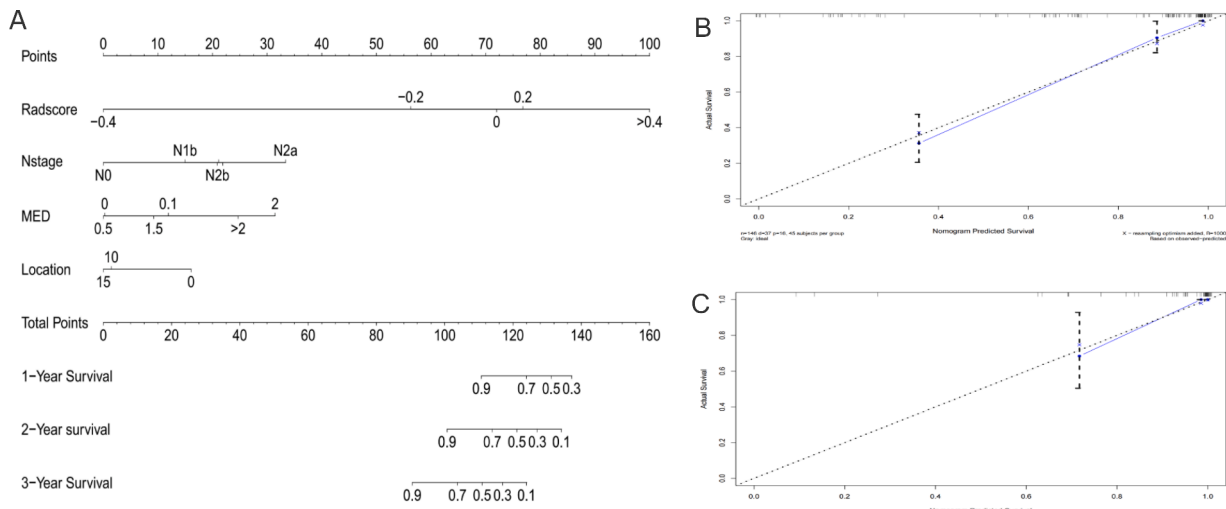


**Fig. 6.** Nomogram for predicting overall survival in patients with rectal cancer (A) and the nomogram calibration curves developed in the training cohorts (B) and validation (C) cohorts.

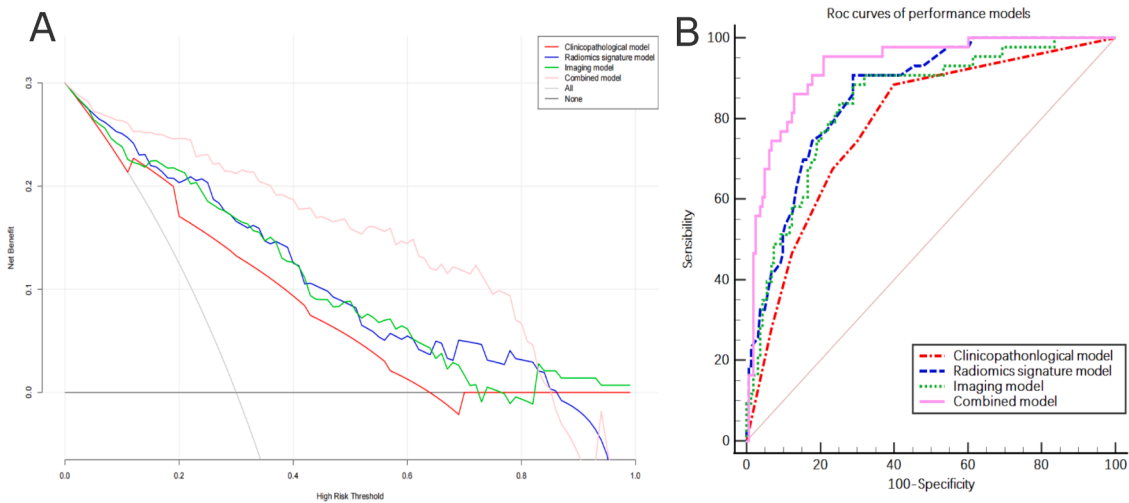


**Fig. 7.** (A) Decision curve analysis for each model, where the y axis represents the net benefit, and the x axis represents the threshold probability. (B) Discriminant performance of all models, showing the receiver-operating characteristic curve and the area under this curve for each of the models at different time points.

**Kaplan-Meier analysis**

Four significant prognostic factors were examined in a Cox regression model. The following cutoff values used to divide high-risk and low-risk groups were obtained: N stage >N0, tumor location ≤ 5 cm, MED > 0.45 cm, and Rad-score > -0.02. Kaplan-Meier analysis was performed to establish their prognostic value. At the same time, the comprehensive model was divided into a low-risk (≤ 0.148) and high-risk group (> 0.148) by calculating the cutoff value. The Kaplan-Meier curves showed that all factors in the high-risk group were significantly correlated with poor OS (Fig. 8).

**Discussion**

Medical image evaluation is a hot topic in precision medicine. Medical imaging technology can provide a considerable amount of non-invasive information regarding pre-treatment evaluation and prediction of a curative effect to guide clinical practice, including treatment. Previous literature included more morphological characteristics of tumors before treatment and combined with MRI-T2WI radiomics features as a prognostic factor for analysis. Our analysis not only confirmed the

prognostic value of this model in patients with rectal cancer but also allowed us to develop and verify a comprehensive model in the form of a radiomics nomogram. Nomograms have a strong predictive ability regarding risk stratification and are optimal for predicting OS in patients with rectal cancer [21,22,32–34]. In this study, we confirmed the value of a nomogram for rectal cancer that had been used successfully to predict survival in patients with other malignant tumors in a validation cohort. It is a useful method for predicting individualized results by calculating the corresponding score and drawing a vertical line down the total component table to obtain the corresponding probability of OS. Therefore, our nomogram, which combines three separate models, can be used as a tool to screen for patients with rectal cancer who have a poor prognosis and to design personalized treatment and follow-up plans for these patients.

The radiomics model constructed by extracting features from T2WI predicted an area under the curve of 0.862 (95% CI 0.808–0.906) for OS, with C-index values of 0.809 and 0.847 in the training and validation cohorts, respectively, which were higher than those calculated for the clinicopathological and tumor morphology models. Patients could be divided into high-risk and low-risk groups based on the Rad-score calculated by the radiomics tag and may have different prognostic

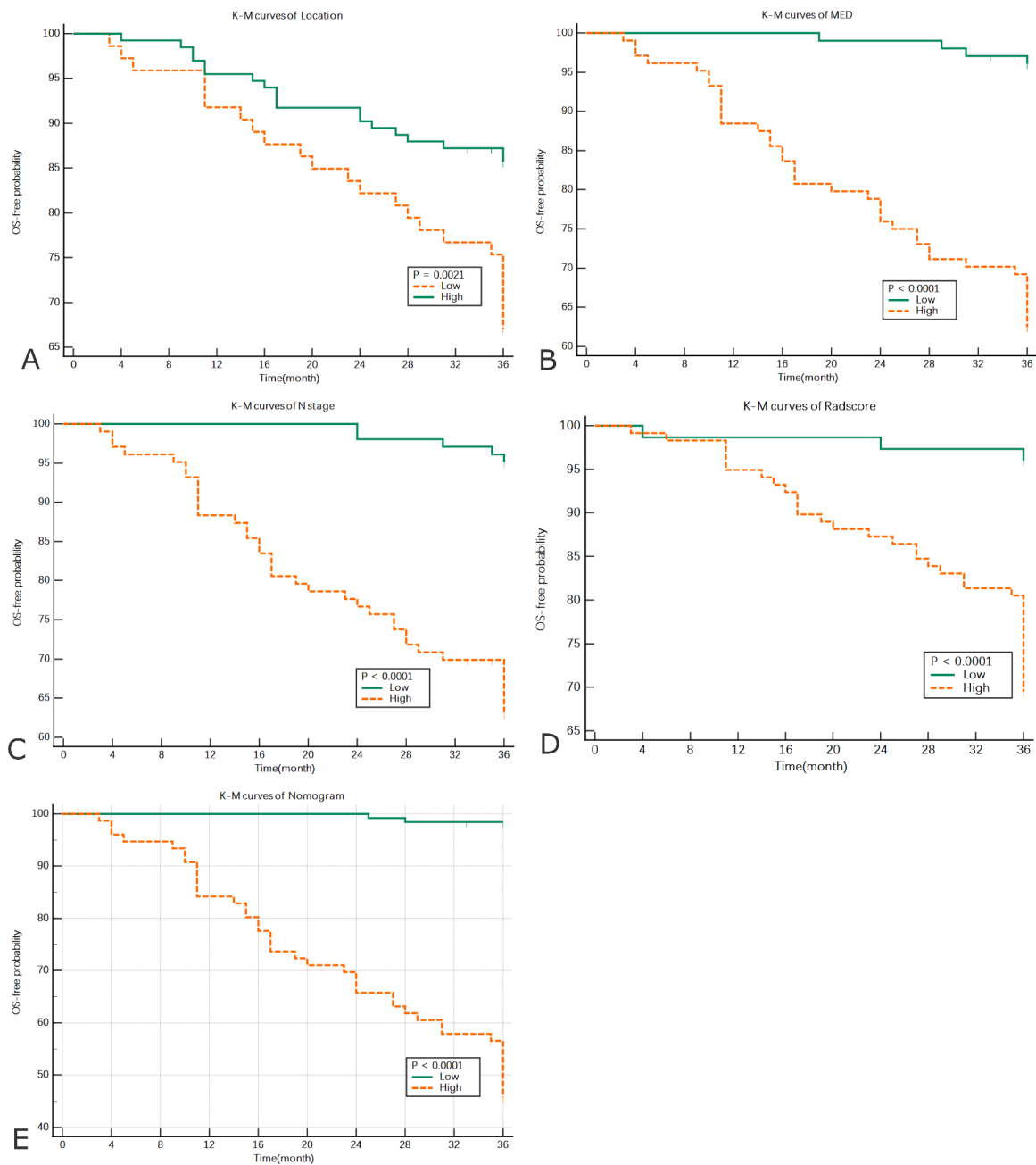


**Fig. 8.** Kaplan-Meier analysis of each prognostic factor in the high-risk group (orange line) and low-risk group (green line). (A) Distance between the lower margin of the tumor and the anal margin, (B) mesorectal extension depth, (C), N stage, (D) Rad-score, and (E) Kaplan-Meier curves for the high-risk and low-risk groups in the nomogram.

outcomes. Our radiomics model includes information obtained by observing the entire tumor and extracting high-dimensional features (such as wavelet and LoG). One of the advantages of radiomics is that it can capture information for the whole tumor rather than for only a slice or certain level in the tumor. Therefore, it reflects the heterogeneity of the tumor as a whole and provides more information than can be obtained from a single section and can be mined for more prognostic information than would be gleaned from clinical factors alone [34,35]. Ten of 1781 radiomics features were found to predict OS, with the wavelet filter contributed the most information ( $n = 6$ ), followed by LoG ( $n = 1$ ), square ( $n = 1$ ), gradient ( $n = 1$ ), and logarithm ( $n = 1$ ). These findings indicate that the wavelet filter contains the most prognostic information and is the best radiomics feature available (three-fifths), in line with the results of other MRI-based radiomics studies [21,24,36].

Wavelet features reflect multi-frequency information for Multiple dimensions of the tumor. LoG reflects tumor information in three frequency domains; the square reflects the square of the image intensities; the gradient reflects the changes in the gradient of voxels in the image; the logarithm reflects the logarithm of the absolute value of the original image+1. Tumor heterogeneity was quantified using these five filters. In this study, the first-order radiomics features had a good classification effect, accounting for one-third of the ten key radiomics features.

Statistical analysis of first-order radiomics features is based on the global grayscale histogram. In our study, the maximum value was for the maximum gray value intensity in the ROI. Skewness and kurtosis describe the shape of the intensity distribution of the data, and skewness reflects an asymmetric data distribution curve to the left (negative skew, below the mean) or the right (positive skew, above the mean). Kurtosis

reflects the distribution position of the “peak” in the ROI. Higher kurtosis means that the quality of the distribution of values is concentrated in the tail rather than the average value, while lower kurtosis means that the quality of the distribution is concentrated on the peak value close to the average value. The results showed that Sub-features: the smaller the value of Maximum (the Wavelet), Kurtosis (the gradient), and Skewness (the Square), the worse the prognosis is.

GLSZM ( $n = 2$ ), NGTDM ( $n = 2$ ), GLRLM ( $n = 1$ ), and GLCM ( $n = 2$ ) are high-order features. GLSZM quantifies the grayscale region in the image, which is defined as the number of adjacent voxels with the same gray intensity. The significant sub-feature of GLSZM in this study are GrayLevelVariance and SmallAreaLowGrayLevelEmphasis. The GrayLevelVariance represents the variance in grayscale intensity in the region. The SmallAreaLowGrayLevelEmphasis measures the proportion in the image of the joint distribution of smaller size zones with lower gray-level values. NGTDM represents the difference between the grayscale value in a certain area and the average grayscale value in the neighboring area. The meaningful sub-features of NGTDM is Complexity, which reflects the degree of unevenness in the image and fast gray change. GLRLM quantifies gray level runs, defined as the length in number of consecutive pixels that have the same gray level value. GLRLM features assess the percentage of pixels/voxels within the ROI, which reflects “graininess.” The meaningful sub-features of GLRLM is LongRunLowGrayLevelEmphasis, which measures the joint distribution of long run lengths with lower gray-level values. GLCM is a second-order grayscale histogram that captures the spatial relationships of pixel/voxel pairs with pre-defined grayscale intensities, in different directions, and with pre-defined distances between pixels/voxels. The significant sub-feature in GLCM is correlation, which is a value between 0 (uncorrelated) and 1 (perfectly correlated), showing the linear dependency of gray level values to their respective voxels in the GLCM. In CLCM, the feature most frequently used in previous radiomics studies is Entropy, which reflects a measure of grayscale heterogeneity/randomness. In this study, we did not extract this feature. This may be due to the sequence we used. The MRI enhanced sequence strongly correlates with the feature Entropy because the characteristics of the uneven enhancement of the tumor precisely reflect the gray heterogeneity of the feature Entropy [19]. The results showed that Sub-features: the smaller the value of GrayLevelVariance (the Wavelet), Complexity (the Wavelet) and Correlation (the Log), the worse the prognosis is, and the higher the value of SmallAreaLowGrayLevelEmphasis (the Wavelet), LongRunLowGrayLevelEmphasis (the Wavelet) and Correlation (the logarithm), the worse the prognosis is.

The area under the curve predicted by the MRI-based tumor morphological model for OS was 0.800 (0.746–0.854). The C-index was 0.793 for the training cohort and 0.835 for the validation cohort, which was better than the traditional clinicopathological model, as in previous studies [37–40]. In this study, the morphological parameters that were statistically significant in univariate analysis were tumor location, tumor length, MED, and CRM, all of which are known to be important prognostic factors. Lower tumor location, a greater tumor length, deeper mesorectum invasion, and a positive CRM are associated with a poor prognosis. Multivariate analysis showed that tumor location and MED had independent prognostic ability. We did not distinguish the location of the tumor according to whether it was in the upper, middle, or lower segment. However, we measured the distance between the lower margin of the tumor and the anal margin accurately. We obtained a risk value of  $\leq 5$  cm, which is similar to the value of 7 cm in a study by Kim et al. [41] and the value of 5 cm reported by Taylor et al. [42]. The mesorectum size was different in different locations of the rectum. The lower the rectum, the positive rate of CRM may also be higher. NCCN rectal cancer guidelines recommend that preoperative neoadjuvant therapy should be performed in patients with T3 ~ 4 stages rectal cancer to reduce tumor staging and increase negative CRM rate. Therefore, preoperative rigorous imaging for accurate assessment of tumor risk in different locations is important for R0 resection rate and reduction of local

recurrence rate. The closer the tumor is to the anal margin, the higher the prognostic risk (HR 01.843, 95% CI 1.960–15.572). MED is an important prognostic factor in patients with rectal cancer, reflecting the invasive nature of the tumor. Previous studies have defined MED as a T3 substage [37,38] (T3a,  $< 1$  mm; T3b, 1–5 mm; T3c,  $> 5$ –10 mm, and T3d,  $> 10$  mm). Survival analysis showed that when the definition was  $> 45$  mm, the survival rate decreased sharply from 96% to 62%, similar to a previous report [38]. T3c and T3d were high-risk groups ( $> 5$  mm). The survival rate was 87% in the low-risk group and approximately 40% in the high-risk group (T3a and T3b,  $< 5$  mm). Therefore, higher MED values are associated with unfavorable tumor characteristics, such as poor differentiation, resulting in a poor prognosis, which is supported by the findings of another study [43].

Given the high number of clinicopathological factors study included in this study, it is surprising that the N stage was the only significant prognostic factor identified in multivariate analysis, in which the N1c stage is a special stage, defined as the N stage of tumor deposition without metastatic lymph nodes, as well as tumor deposition in the pathological report as a prognostic factor. However, like some other factors, it was not meaningful in univariate analysis, which is not consistent with previous reports [7,43]. Moreover, the significance of CEA and CA199 in this prognostic study was also not shown. In contrast, Huh et al. [44] and Jeong et al. [45] found that a postoperative CEA level  $\leq 2.5$  ng/ml predicted a lower postoperative recurrence rate and less risk of distant metastasis of rectal cancer. For CA199, although other studies have defined the positive value of CA199 to be 27 U/ml or 37 U/ml [37,43]; however, a level of 20 U/ml was associated with greater risk in the study by Cui et al. [21] further research is needed to confirm this idea.

This study had some limitations. First, we only extracted radiomics features from a single sequence T2WI. Although T2WI has the best performance [33], it provides limited information. Future studies should include multi-parameter MRI, such as diffusion-weighted imaging, the apparent diffusion coefficient, and enhanced sequences. Previous studies have performed radiomics analysis of polyphasic enhancement sequences, diffusion-weighted images, and apparent diffusion coefficient sequences, in which enhanced sequence images can provide better tissue contrast for delineation of a tumor and more information about tumor heterogeneity. Combining these imaging methods can improve the predictive ability [21,34,46,47] and may even include pathological and molecular imaging to build a more comprehensive and stable prediction model.

Second, tumor delineating is the most important aspect of the radiomics workflow. Although it is an analysis of the whole lesion, the potential changes in the delineation process also affect the extracted feature. The motion of the tumor caused by intestinal peristalsis is one of the factors leading to the variation of radiomics features. When the image is blurred, or the artifacts are large, the gray value and the spatial distribution of the pixels in the ROI change. Therefore, the patients should be instructed to prepare the intestine before imaging to restrain the intestinal peristalsis. In addition, in 206 T2WI images, the uncertain boundary between the edge of the tumor and the normal intestinal wall was excluded to improve the stability of feature extraction. ICC is needed to observe the repeatability of the extracted image features. When the feature ICC  $> 0.8$ , it can be included in the study. It is time-consuming and laborious to delineate tumors manually, so automatic delineation is a promising solution, but its accuracy and stability still need improvement. Improving the segmentation algorithm is worth further research to promote the efficiency of the use of imageology in busy clinical practice. It is worth mentioning that the scanning equipment, image acquisition, post-processing schemes, analysis software, and research methods used in each research have not been fully standardized, resulting in low standardization and repeatability of results.

The third limitation is that the follow-up period was relatively short in that we built a predictive model based only on 3-year OS. Future studies should extend the follow-up period to 5 years. The fourth

limitation is that the study lacked external validation. However, we evaluated the clinical effectiveness of the comprehensive model using DCA and confirmed that its incremental value over and above the clinicopathological model could be used for personalized estimation of risk. Multicenter centers are needed in the future to assess the generalizability of our experimental results.

Many published predictive models can consider factors related to disease and treatment, but these models lack standardized evaluation of their performance, repeatability, and/or clinical practicality. Therefore, these models may not be suitable for clinical-decision support systems (CDSS), but radiomics can still be used to assist other factors to improve medical decision-making [48]. Although there has not been a standardized report on imageology in the world, in a comparative study on the construction of a model of Imageology, the models constructed by young and experienced physicians were evaluated with good agreement between the two groups. The results show that the imaging group has a good reproducibility in the same doctors' group, which is beneficial to the popularization of radiology in the group. These results indicate that radiomics has good reproducibility in the same group of doctors, which is conducive to promoting radiometrics in the group of doctors [49].

## Conclusion

This study has identified a novel non-invasive prognostic biomarker based on radiological features that can be identified on MRI scans acquired preoperatively. This biomarker could improve the prognostic ability of clinicopathology and tumor morphology and improve the ability to detect rectal tumors in the early stages of the disease. Our radiomics nomogram successfully divides patients into high-risk and low-risk groups, which would assist with risk stratification and subsequent monitoring. This study affords important insights for precision therapy and provides clinicians with an opportunity to develop personalized strategies for radical surgery, radiotherapy, and chemotherapy designed to improve the prognosis of patients with rectal cancer.

## Copyright

This is an open-access article distributed under the terms of the Creative Commons Attribution License, which permits unrestricted use, distribution, and reproduction in any medium, provided the original author and source are credited.

## Data availability

The authors confirm that all data underlying the findings are fully available without restriction. All relevant data are within the paper and its Supporting Information files.

## CRedit authorship contribution statement

**Zhou Chuanji:** Conceptualization, Investigation, Writing – original draft, Methodology, Software, Visualization, Data curation. **Wang Zheng:** Conceptualization, Investigation, Supervision, Writing – review & editing, Funding acquisition, Validation. **Lai Shaolv:** Supervision, Writing – review & editing, Funding acquisition, Validation. **Meng Linghou:** Supervision, Resources. **Lu Yixin:** Investigation, Resources. **Lu Xinhui:** Investigation, Validation. **Lin Ling:** Investigation, Validation. **Tang Yunjing:** Investigation. **Zhang Shilai:** Investigation. **Mo Shaozhou:** Investigation. **Zhang Boyang:** Investigation.

## Declaration of Competing Interest

The authors declare that they have no known competing financial interests or personal relationships that could have appeared to influence the work reported in this paper.

## Funding

This study was supported by grants from the following institutions: Guangxi Clinical Research Center for Medical Imaging Construction (Grant No. Guike AD20238096); Guangxi Key Clinical Specialty (Medical Imaging Department); Dominant Cultivation Discipline of Guangxi Medical University Cancer Hospital (Medical Imaging Department); Guangxi Medical and Health Appropriate Technology and Popularization and Application Project (Grant No. S2020093). The funders had no role in study design, data collection and analysis, decision to publish, or manuscript preparation.

## Supplementary materials

Supplementary material associated with this article can be found, in the online version, at doi:10.1016/j.tranon.2022.101352.

## References

- [1] J.F. Shi, L. Wang, J.C. Ran, et al., Clinical characteristics, medical service utilization, and expenditure for colorectal cancer in China, 2005 to 2014: overall design and results from a multicenter retrospective epidemiologic survey, *Cancer* 127 (11) (2021) 1880–1893.
- [2] M. Wong, J. Huang, V. Lok, et al., Differences in incidence and mortality trends of colorectal cancer worldwide based on sex, age, and anatomic location, *Clin. Gastroenterol. Hepatol.* 19 (5) (2021) 955–966.
- [3] A.N. Archambault, Y. Lin, J. Jeon, et al., Nongenetic determinants of risk for early-onset colorectal cancer, *JNCI Cancer Spectr.* 5 (3) (2021) b29.
- [4] S.H. Emile, H. Elfeki, M. Shalaby, et al., Patients with early-onset rectal cancer aged 40 year or less have similar oncologic outcomes to older patients despite presenting in more advanced stage; a retrospective cohort study, *Int. J. Surg.* 83 (2020) 161–168.
- [5] J. Silva-Velazco, D.W. Dietz, L. Stocchi, et al., Considering value in rectal cancer surgery: an analysis of costs and outcomes based on the open, laparoscopic, and robotic approach for proctectomy, *Ann. Surg.* 265 (5) (2017) 960–968.
- [6] M. Paku, M. Uemura, M. Kitakaze, et al., Impact of the preoperative prognostic nutritional index as a predictor for postoperative complications after resection of locally recurrent rectal cancer, *BMC Cancer* 21 (1) (2021) 435.
- [7] A.C. Lord, N. D'Souza, A. Shaw, et al., MRI-diagnosed tumour deposits and EMVI status have superior prognostic accuracy to current clinical TNM staging in rectal cancer, *Ann. Surg.* Sep 15 (2020), <https://doi.org/10.1097/SLA.0000000000004499>. Publish Ahead of Print.
- [8] A.B. Benson, A.P. Venook, M.M. Al-Hawary, et al., Rectal cancer, version 2.2018, NCCN clinical practice guidelines in oncology, *J. Natl. Compr. Cancer Netw.* 16 (7) (2018) 874–901.
- [9] E.D. Kennedy, M. Simunovic, K. Jhaveri, et al., Safety and feasibility of using magnetic resonance imaging criteria to identify patients with "good prognosis" rectal cancer eligible for primary surgery: the phase 2 nonrandomized quicksilver clinical trial, *JAMA Oncol.* 5 (7) (2019) 961–966.
- [10] P. Zhou, P. Goffredo, T. Ginader, et al., Impact of KRAS status on tumor response and survival after neoadjuvant treatment of locally advanced rectal cancer, *J. Surg. Oncol.* 123 (1) (2021) 278–285.
- [11] D. Cai, Z.H. Huang, H.C. Yu, et al., Prognostic value of preoperative carcinoembryonic antigen/tumor size in rectal cancer, *World J. Gastroenterol.* 25 (33) (2019) 4945–4958.
- [12] P. Lovinfosse, M. Polus, D. Van Daele, et al., FDG PET/CT radiomics for predicting the outcome of locally advanced rectal cancer, *Eur. J. Nucl. Med. Mol. Imaging* 45 (3) (2018) 365–375.
- [13] J.P. O'Connor, E.O. Aboagye, J.E. Adams, et al., Imaging biomarker roadmap for cancer studies, *Nat. Rev. Clin. Oncol.* 14 (3) (2017) 169–186.
- [14] F. Davnall, C.S. Yip, G. Ljungqvist, et al., Assessment of tumor heterogeneity: an emerging imaging tool for clinical practice? *Insights Imaging* 3 (6) (2012) 573–589.
- [15] Z. Wang, D. Xie, Q. Li, Progress in the application of imaging science in rectal cancer, *J. Clin. Radiol.* 39 (08) (2020) 1662–1665.
- [16] G. Brown, C.J. Richards, R.G. Newcombe, et al., Rectal carcinoma: thin-section MR imaging for staging in 28 patients, *Radiology* 211 (1) (1999) 215–222.
- [17] P. Tripathi, W. Guo, S. Rao, et al., Additional value of MRI-detected EMVI scoring system in rectal cancer: applicability in predicting synchronous metastasis, *Tumori* 106 (4) (2020) 286–294.
- [18] M.E. Mayerhoefer, A. Materka, G. Langa, et al., Introduction to radiomics, *J. Nucl. Med.* 61 (4) (2020) 488–495.
- [19] X.F. Quo, W.Q. Yang, Q. Yang, et al., Feasibility of MRI radiomics for predicting KRAS mutation in rectal cancer, *Curr. Med. Sci.* 40 (6) (2020) 1156–1160.
- [20] Y. Zhang, K. He, Y. Guo, et al., A novel multimodal radiomics model for preoperative prediction of lymphovascular invasion in rectal cancer, *Front. Oncol.* 10 (2020) 457.
- [21] Y. Cui, W. Yang, J. Ren, et al., Prognostic value of multiparametric MRI-based radiomics model: potential role for chemotherapeutic benefits in locally advanced rectal cancer, *Radiother. Oncol.* 154 (2020) 161–169.

- [22] M. Li, Y.Z. Zhu, Y.C. Zhang, et al., Radiomics of rectal cancer for predicting distant metastasis and overall survival, *World J. Gastroenterol.* 26 (33) (2020) 5008–5021.
- [23] N.J. Wesdorp, T. Hellingman, E.P. Jansma, et al., Advanced analytics and artificial intelligence in gastrointestinal cancer: a systematic review of radiomics predicting response to treatment, *Eur. J. Nucl. Med. Mol. Imaging* 48 (6) (2021) 1785–1794.
- [24] J. Fang, B. Zhang, S. Wang, et al., Association of MRI-derived radiomic biomarker with disease-free survival in patients with early-stage cervical cancer, *Theranostics* 10 (5) (2020) 2284–2292.
- [25] S. Dastmalchian, O. Kilinc, L. Onyewadume, et al., Radiomic analysis of magnetic resonance fingerprinting in adult brain tumors, *Eur. J. Nucl. Med. Mol. Imaging* 48 (3) (2021) 683–693.
- [26] M. Kirienko, M. Sollini, M. Corbetta, et al., Radiomics and gene expression profile to characterise the disease and predict outcome in patients with lung cancer, *Eur. J. Nucl. Med. Mol. Imaging* 48(11) (2021) 3643–3655.
- [27] A. Conti, A. Duggento, I. Indovina, et al., Radiomics in breast cancer classification and prediction, *Semin. Cancer Biol.* 72 (2021) 238–250.
- [28] S. Gourtsoyianni, N. Papanikolaou, Role of magnetic resonance imaging in primary rectal cancer-standard protocol and beyond, *Semin. Ultrasound CT MR* 37 (4) (2016) 323–330.
- [29] B. Petresc, A. Lebovici, C. Caraiani, et al., Pre-treatment T2-WI based radiomics features for prediction of locally advanced rectal cancer non-response to neoadjuvant chemoradiotherapy: a preliminary study, *Cancers* 12 (7) (2020) 1894 (Basel).
- [30] M. Liang, Z. Cai, H. Zhang, et al., Machine learning-based analysis of rectal cancer mri radiomics for prediction of metachronous liver metastasis, *Acad. Radiol.* 26 (11) (2019) 1495–1504.
- [31] J.J.M. van Griethuysen, A. Fedorov, C. Parmar, et al., Computational radiomics system to decode the radiographic phenotype, *Cancer Res.* 77 (21) (2017) e104–e107.
- [32] Y. Meng, Y. Zhang, D. Dong, et al., Novel radiomic signature as a prognostic biomarker for locally advanced rectal cancer, *J. Magn. Reson. Imaging* (Online ahead of print) (2018), <https://doi.org/10.1002/jmri.25968>.
- [33] Z.Y. Li, X.D. Wang, M. Li, et al., Multi-modal radiomics model to predict treatment response to neoadjuvant chemotherapy for locally advanced rectal cancer, *World J. Gastroenterol.* 26 (19) (2020) 2388–2402.
- [34] C. Cai, T. Hu, J. Gong, et al., Multiparametric MRI-based radiomics signature for preoperative estimation of tumor-stroma ratio in rectal cancer, *Eur. Radiol.* 31(5) (2020) 3326–3335.
- [35] D. Cai, X. Duan, W. Wang, et al., A metabolism-related radiomics signature for predicting the prognosis of colorectal cancer, *Front. Mol. Biosci.* 7 (2020), 613918.
- [36] Z. Li, X. Ma, F. Shen, et al., Evaluating treatment response to neoadjuvant chemoradiotherapy in rectal cancer using various MRI-based radiomics models, *BMC Med. Imaging* 21 (1) (2021) 30.
- [37] T. Tong, Z. Yao, L. Xu, et al., Extramural depth of tumor invasion at thin-section MR in rectal cancer: associating with prognostic factors and ADC value, *J. Mag. Reson. Imaging* 40 (3) (2014) 738–744.
- [38] L.S. Lino-Silva, R. Loeza-Belmont, M.A. Gomez Alvarez, et al., Mesorectal invasion depth in rectal carcinoma is associated with low survival, *Clin. Colorectal Cancer* 16 (1) (2017) 73–77.
- [39] J.S. Bae, S.H. Kim, B.Y. Hur, et al., Prognostic value of MRI in assessing extramural venous invasion in rectal cancer: multi-readers' diagnostic performance, *Eur. Radiol.* 29 (8) (2019) 4379–4388.
- [40] J.J. van den Broek, F.S.W. van der Wolf, L.A. Heijnen, et al., The prognostic importance of MRI detected extramural vascular invasion (mrEMVI) in locally advanced rectal cancer, *Int. J. Colorectal Dis.* 35 (10) (2020) 1849–1854.
- [41] C.H. Kim, J.W. Huh, S.S. Yeom, et al., Predictive value of serum and tissue carcinoembryonic antigens for radiologic response and oncologic outcome of rectal cancer, *Pathol. Res. Pract.* 216 (3) (2020), 152834.
- [42] F.G. Taylor, P. Quirke, R.J. Heald, et al., Preoperative magnetic resonance imaging assessment of circumferential resection margin predicts disease-free survival and local recurrence: 5-year follow-up results of the MERCURY study, *J. Clin. Oncol.* 32 (1) (2014) 34–43.
- [43] O. Benoit, M. Svrcek, B. Creavin, et al., Prognostic value of tumor deposits in rectal cancer: a monocentric series of 505 patients, *J. Surg. Oncol.* 122 (7) (2020) 1481–1489.
- [44] J.W. Huh, S.H. Yun, S.H. Kim, et al., Prognostic role of carcinoembryonic antigen level after preoperative chemoradiotherapy in patients with rectal cancer, *J. Gastrointest. Surg.* 22 (10) (2018) 1772–1778.
- [45] S. Jeong, T.K. Nam, J.U. Jeong, et al., Postoperative carcinoembryonic antigen level has a prognostic value for distant metastasis and survival in rectal cancer patients who receive preoperative chemoradiotherapy and curative surgery: a retrospective multi-institutional analysis, *Clin. Exp. Metastasis* 33 (8) (2016) 809–816.
- [46] H.T. Zhu, X.Y. Zhang, Y.J. Shi, et al., A deep learning model to predict the response to neoadjuvant chemoradiotherapy by the pretreatment apparent diffusion coefficient images of locally advanced rectal cancer, *Front. Oncol.* 10 (2020), 574337.
- [47] L. Wan, W. Peng, S. Zou, et al., MRI-based delta-radiomics are predictive of pathological complete response after neoadjuvant chemoradiotherapy in locally advanced rectal cancer, *Acad. Radiol. Suppl* 1 (2020) S95–S104.
- [48] P. Lambin, R.T.H. Leijenaar, T.M. Deist, et al., Radiomics: the bridge between medical imaging and personalized medicine, *Nat. Rev. Clin. Oncol.* 14 (12) (2017) 749–762.
- [49] J. van Griethuysen, D. Lambregts, S. Trebeschi, et al., Radiomics performs comparable to morphologic assessment by expert radiologists for prediction of response to neoadjuvant chemoradiotherapy on baseline staging MRI in rectal cancer, *Abdom. Radiol.* 45 (3) (2020) 632–643 (NY).